

Technical report 09-058

Optimization of Condition-Based Asset Management Using a Predictive Health Model*

G. Bajracharya, T. Koltunowicz, R. R. Negenborn, Z. Papp,
D. Djairam, B. De Schutter, and J. J. Smit

To cite this work, please refer to the published version:

G. Bajracharya, T. Koltunowicz, R. R. Negenborn, Z. Papp, D. Djairam, B. De Schutter, and J. J. Smit, "Optimization of condition-based asset management using a predictive health model," *Proceedings of the 16th International Symposium on High Voltage Engineering*, Cape Town, South Africa, pp. 1529–1534, Aug. 2009.

Delft Center for Systems and Control
Delft University of Technology
Mekelweg 2, 2628 CD Delft
The Netherlands
phone: +31-15-278.24.73 (secretary)
URL: <https://www.dcsc.tudelft.nl>

* This report can also be downloaded via <https://dpub.eu/09-058>

Optimization of Condition-Based Asset Management Using a Predictive Health Model

G. Bajracharya^{1*}, T. Koltunowicz¹, R. R. Negenborn², Z. Papp⁴,
D. Djairam¹, B. De Schutter^{2,3} and J. J. Smit¹

¹ Department of High-Voltage Components and Power Systems,
Delft University of Technology, P.O. Box 5031, 2600 GA Delft, The Netherlands

² Delft Center for Systems and Control,

³ Department of Marine and Transport Technology,
Delft University of Technology, Mekelweg 2, 2628 CD Delft, The Netherlands

⁴ TNO Science and Industry,

P.O. Box 155, 2600 AD Delft, The Netherlands

* Email: g.bajracharya@tudelft.nl

Abstract: In this paper, a model predictive framework is used to optimize the operation and maintenance actions of power system equipment based on the predicted health state of this equipment. In particular, this framework is used to predict the health state of transformers based on their usage. The health state of a transformer is hereby given by the hot-spot temperature of the paper insulation of the transformer and is predicted using the planned loading of the transformer. The actual loading of the transformer is subsequently optimized using these predictions.

1 Introduction

With a significant portion of the electrical infrastructure reaching the end of its operational age within the coming few decades, reliability of the electricity grid is becoming a more and more important issue. The reliability of the grid can be improved by monitoring its condition and by taking preventive actions based on this condition [1]. Currently, condition-based asset management is based mainly on historic data and on heuristics. In order to optimize the operation and maintenance of power system equipment, while assuring a predefined level of reliability, a model describing the evolution of its health state, has to be incorporated into the asset management [2].

In [2], a framework is proposed for modeling the health state of power system equipment and used for modeling degradation of the paper insulation of transformers. The framework can be used to predict the effects of different maintenance actions and usage patterns. The predictions can then be used for the optimization of maintenance actions and the equipment usage. In this paper, we use this framework to optimize the loading of the transformer using temperature predictions.

The loading limits of a transformer depend on the temperature within that transformer. The so-called hot-spot temperature can therefore be used to determine the loading limits [3,4]. This hot-spot temperature can be predicted using the load of the transformer [3-7].

2 Framework for model-based optimization

A framework for model-based optimization using a predictive health model has been proposed in [2]. Using this predictive health model, the future health state of equipment that is used in the electricity grid can be predicted given a range of possible actions and usage patterns of its equipment. The framework also defines the cost function for the optimization. Below the components of this framework are outlined briefly.

2.1 Predictive health model

The predictive health model in the framework consists of a dynamic stress model, a failure model and an estimation of cumulative stresses, as illustrated

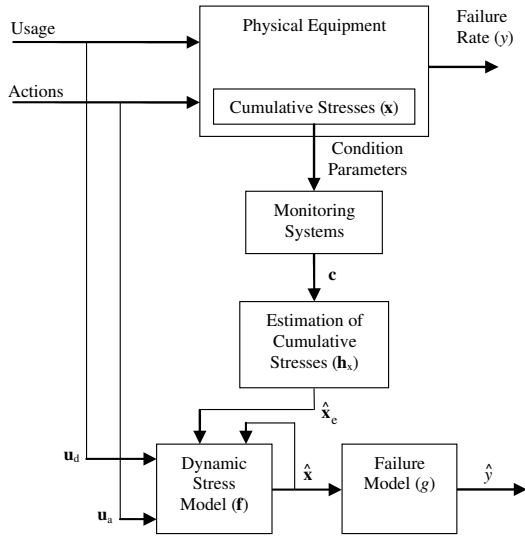


Figure 1: Predictive health model which predicts cumulative stresses and failure rate for the given usage and actions.

in Figure 1. As equipment ages, various stresses, such as electrical, thermal, mechanical and environmental stresses, weaken the strength of the equipment. The cumulative stresses of the equipment are affected by the usage pattern (e.g., the loading) and the maintenance actions (e.g., the replacement of parts) performed on the equipment. The health state of the equipment is represented by the cumulative stresses. Their dynamics can be described using a dynamic stress model such as the following discrete-time state-space model:

$$\hat{\mathbf{x}}(k+1) = \mathbf{f}(\hat{\mathbf{x}}(k), \mathbf{u}(k)) \quad , \quad (1)$$

where $\mathbf{u}(k) = [\mathbf{u}_a(k) \quad \mathbf{u}_d(k)]^T$. At discrete time step k , the future cumulative stresses $\hat{\mathbf{x}}(k+1)$ are predicted based on the usage of the equipment $\mathbf{u}_d(k)$, the maintenance actions $\mathbf{u}_a(k)$ and the current cumulative stresses $\hat{\mathbf{x}}(k)$.

As the cumulative stresses increase over time, the probability of failure of the equipment also increases. The relationship between the cumulative stresses and the failure rate of the equipment is described in a failure model. The failure model uses the predicted cumulative stresses to predict the failure rate of the equipment. The failure model directly maps the cumulative stresses to the failure rate $\hat{y}(k)$ as follows:

$$\hat{y}(k) = g(\hat{\mathbf{x}}(k)) \quad . \quad (2)$$

The cumulative stresses are indicated by condition parameters of the equipment, such as the partial

discharge, temperature measurements, etc. Different online and offline monitoring systems can detect these condition parameters. In practice, only a few condition parameters (such as the electrical and thermal stresses) are measured by monitoring systems. Estimates of the monitored cumulative stresses $\hat{\mathbf{x}}_e(k)$ can be made based on measurements $\mathbf{c}(k)$ of the monitoring systems as follows:

$$\hat{\mathbf{x}}_e(k) = \mathbf{h}_x(\mathbf{c}(k)) \quad . \quad (3)$$

The obtained cumulative stress estimates $\hat{\mathbf{x}}_e$ can be used in the dynamic stress model to update the corresponding cumulative stresses. The remaining unmonitored cumulative stresses are predicted by the dynamic stress model.

The framework of the predictive health model can be used to predict the health state and the failure rate of equipment by considering its usage and the performed maintenance actions. The measurements of the monitoring systems can be used to update the cumulative stresses of the equipment.

2.2 Optimization of maintenance and usage

Typically, maintenance improves the health state of the equipment, which, in turn, reduces its failure rate. An optimal maintenance action balances the economical cost of the maintenance, the improvement of the health state and the reduction in the failure rate of the equipment. The usage indicates its utilization.

The process of model-based optimization is illustrated in Figure 2. The total cost of the usage and the maintenance actions is defined to consist of three sub-cost functions. The sub-cost function of the planned usage and the maintenance actions J_a incorporates the economical cost of the maintenance. The sub-cost function of the failure rate J_f takes into account the cost associated with the failure of the equipment. The sub-cost function of the cumulative stresses J_{cs} incorporates the cost of the deterioration of the equipment. The summation of these three sub-cost functions gives the total cost of a particular maintenance action in a particular state.

The optimization of the usage and the maintenance actions is considered over a given predicted time frame of N steps in the future, such that future usage and future maintenance actions can be optimized. The total cost over the predicted time frame is considered in the optimization. Hence, the model-based optimization problem is formulated as

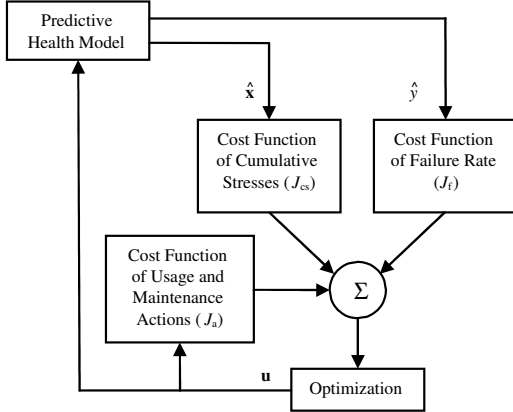


Figure 2: Optimization of maintenance. Cost functions are associated with cumulative stresses, failure rate and usage and maintenance actions.

follows:

$$\min_{\mathbf{u}(k), \dots, \mathbf{u}(k+N-1)} \left[\sum_{l=0}^{N-1} J_a(\mathbf{u}(k+l)) \right] + \left[\sum_{l=0}^{N-1} J_f(\hat{\mathbf{y}}(k+l)) \right] + J_{cs}(\hat{\mathbf{x}}(k+N) - \hat{\mathbf{x}}(k)) \quad (4)$$

subject to

$$\begin{aligned} \hat{\mathbf{x}}(k+l+1) &= \mathbf{f}(\hat{\mathbf{x}}(k+l), \mathbf{u}(k+l)) \\ \hat{\mathbf{y}}(k+l) &= \mathbf{g}(\hat{\mathbf{x}}(k+l)) \quad \text{for } l = 0, \dots, N-1. \end{aligned}$$

The predictive health model is thus used to predict the cumulative stresses and the failure rates for the planned usage pattern and different future maintenance actions. The total cost is evaluated for different future usage and maintenance actions over the predicted time frame. In this way, the optimal usage and maintenance actions minimizing the total cost over the time horizon is searched for.

3 Thermal effects in a power transformer

Temperatures within a transformer are important factors for its operation. Below we discuss the different types of temperatures that play a role and their consequences for transformer loading requirements.

3.1 Temperatures in a transformer

The main sources of the heat generated within a transformer are losses in its magnetic core and in

Table 1: Suggested maximum temperature of loading types based on the hot-spot temperature [4].

| Loading types | Maximum hot-spot temperature (°C) |
|----------------------------------|-----------------------------------|
| Normal life expectancy loading | 120 |
| Planned loading beyond nameplate | 130 |
| Long-time emergency loading | 140 |
| Short-time emergency loading | 180 |

its windings. The core losses depend on the applied voltage of the transformer; the winding losses depend on the loading (current) of the transformer. Other stray losses (constituting losses due to the leakage flux, the winding connection, and the terminal connections) also contribute to the heating of the transformer. In the case of an oil-immersed transformer, the heat dissipated in the core, the windings, and the other parts is transferred to the oil. Subsequently, the heat is transferred from the oil to the cooling medium via the radiators.

The winding material in a transformer can withstand temperatures of several hundred degrees Celsius and the oil does not degrade significantly below 140 °C [7]. However, insulation paper that surrounds the windings in a transformer degrades increasingly rapid as the temperature exceeds 90 °C. This degradation process reduces the dielectric and mechanical strength of the insulation paper and hence reduces its life time [2-4,8].

Different temperatures inside the transformer are defined, as illustrated in Figure 3. The hot-spot temperature is defined as the temperature of the hottest part of the windings. It is this temperature that is used for determining the level of the paper degradation.

3.2 Loading of transformers

The maximum allowable loading of a transformer mainly depends on the thermal performance of the transformer. IEEE C57.91 [4] defines four types of loading, for which the suggested maximum hot-spot temperature is given in Table 1.

Under normal life expectancy loading, the maximum hot-spot temperature allowed is 120 °C. The planned loading beyond nameplate is suggested for a planned, repetitive load, provided that the transformer is not loaded continuously at the rated load. The long-time emergency loading is suggested only for rare emergency conditions. The short-time emergency loading is only suggested for a short time in

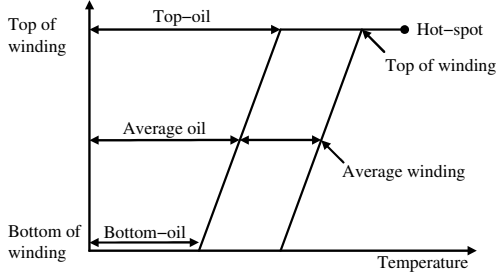


Figure 3: Different temperatures and their location within the transformer [3,7].

a few abnormal emergency conditions. Normal life expectancy loading is considered risk free [4]. In the other three cases, the calculation of the loss of life due to the loading and the risk of failure associated with this should be considered.

4 Thermal model of a power transformer

The thermal models of a power transformer are based on the ambient temperature, the top-oil or bottom-oil temperatures, and the hot-spot temperature. The oil temperatures are calculated based on the ambient temperature and on the dynamics of the heat transfer from the oil to the environment through the radiators. Similarly, the hot-spot temperature is calculated based on the oil temperatures and on the dynamics of the heat transfer between the windings and the oil.

IEEE C57.91 [4] suggests a top-oil time constant based on the mass of different parts and on the cooling type of the transformer. The winding time constant, which describes the dynamics of the heat transfer between the windings and the oil, is estimated based on the cooling experiments. Swift et al. [5] propose a thermal model based on heat transfer theory, which includes thermal capacitances and non-linear thermal resistances. Their approach is extended by Susa et al. [6,7] by considering the oil viscosity changes and the loss variation with the temperature. Their thermal model consists of the top-oil model and the hot-spot model, as presented below.

4.1 Top-oil thermal model

The top-oil temperature depends on the load factor and the ambient temperature. The dynamics of the

top-oil temperature θ_{oil} are described by:

$$\begin{aligned} & \frac{1 + R \cdot K^2}{1 + R} \cdot (\mu_{pu}(\theta_{oil}))^n \cdot \Delta\theta_{oil,rated} \\ &= (\mu_{pu}(\theta_{oil}))^n \cdot \tau_{oil,rated} \cdot \frac{d\theta_{oil}}{dt} + \frac{(\theta_{oil} - \theta_{amb})^{n+1}}{(\Delta\theta_{oil,rated})^n}, \end{aligned} \quad (5)$$

where θ_{amb} is the ambient temperature, K is the load factor (the per unit (pu) load), R is the ratio of load losses at the rated current and no-load losses, $\Delta\theta_{oil,rated}$ is the rated top-oil temperature rise over the ambient temperature, $\mu_{pu}(\theta_{oil})$ is the variable oil viscosity in pu, $\tau_{oil,rated}$ is the rated top-oil time constant and n is a constant which depends on the type of cooling.

The rated top-oil time constant $\tau_{oil,rated}$ (in minutes) can be calculated as:

$$\tau_{oil,rated} = \frac{0.48 \cdot M_{FLUID} \cdot \Delta\theta_{oil,rated}}{P} \cdot 60, \quad (6)$$

where M_{FLUID} is the mass of the oil in kg and P represents the total losses at the rated load in watts.

The change in viscosity of oil at the top-oil temperature $\mu_{pu}(\theta_{oil})$ is given by:

$$\mu_{pu}(\theta_{oil}) = \frac{\exp(2797.3 / (\theta_{oil} + 273))}{\exp(2797.3 / (\theta_{oil,rated} + 273))}, \quad (7)$$

where $\theta_{oil,rated}$ is the rated top-oil temperature.

4.2 Hot-spot thermal model

The hot-spot temperature θ_{hs} is based on the top-oil temperature and the load factor. Its dynamics are described as follows:

$$\begin{aligned} & K^2 \cdot P_{cu,pu}(\theta_{hs}) \cdot (\mu_{pu}(\theta_{oil}))^n \cdot \Delta\theta_{hs,rated} \\ &= (\mu_{pu}(\theta_{oil}))^n \cdot \tau_{wdg,rated} \cdot \frac{d\theta_{hs}}{dt} + \frac{(\theta_{hs} - \theta_{oil})^{n+1}}{(\Delta\theta_{hs,rated})^n}, \end{aligned} \quad (8)$$

where $\Delta\theta_{hs,rated}$ is the rated hot-spot temperature rise over the top-oil temperature, $P_{cu,pu}(\theta_{hs})$ are the variable load losses in pu and $\tau_{wdg,rated}$ is the rated hot-spot time constant. The variable load losses $P_{cu,pu}(\theta_{hs})$ is given by:

$$\begin{aligned} P_{cu,pu}(\theta_{hs}) &= P_{cu,dc,pu} \frac{235 + \theta_{hs}}{235 + \theta_{hs,rated}} \\ &+ P_{cu,eddy,pu} \frac{235 + \theta_{hs,rated}}{235 + \theta_{hs}}, \end{aligned} \quad (9)$$

where $P_{cu,dc,pu}$ are the DC losses in pu, $P_{cu,eddy,pu}$ are the eddy current losses in pu and $\theta_{hs,rated}$ is the rated hot-spot temperature.

5 Thermal model in the model-based optimization framework

The thermal models (5), (8) are converted to the dynamic stress model (1) of the model-based optimization framework. The top-oil temperature θ_{oil} and the hot-spot temperature θ_{hs} are taken as cumulative stresses $x_{\theta,oil}$ and $x_{\theta,hs}$, respectively. The load factor K is taken as the usage u_I . The ambient temperature θ_{amb} is taken as the exogenous input $u_{\theta,amb}$. The differential equations (5) and (8) are discretized by using the forward Euler approximation. The top-oil model discretized from (5) is then given by:

$$\begin{aligned} & \frac{1+R \cdot (u_I(k))^2}{1+R} \cdot (\mu_{pu}(k))^n \cdot \Delta\theta_{oil,rated} \\ &= (\mu_{pu}(k))^n \cdot \tau_{oil,rated} \cdot \frac{x_{\theta,oil}(k+1) - x_{\theta,oil}(k)}{h} \\ &+ \frac{(x_{\theta,oil}(k) - u_{\theta,amb}(k))^{n+1}}{(\Delta\theta_{oil,rated})^n}, \end{aligned} \quad (10)$$

where h is the time step and

$$\mu_{pu}(k) = \frac{\exp(2797.3 / (x_{\theta,oil}(k) + 273))}{\exp(2797.3 / (\theta_{oil,rated} + 273))}. \quad (11)$$

The discretized hot-spot model is then given by:

$$\begin{aligned} & (u_I(k))^2 \cdot P_{cu,pu}(k) \cdot (\mu_{pu}(k))^n \cdot \Delta\theta_{hs,rated} \\ &= (\mu_{pu}(k))^n \cdot \tau_{wdg,rated} \cdot \frac{x_{\theta,hs}(k+1) - x_{\theta,hs}(k)}{h} \\ &+ \frac{(x_{\theta,hs}(k) - x_{\theta,oil}(k))^{n+1}}{(\Delta\theta_{hs,rated})^n}, \end{aligned} \quad (12)$$

where

$$\begin{aligned} P_{cu,pu}(k) &= P_{cu,dc,pu} \frac{235 + x_{\theta,hs}(k)}{235 + \theta_{hs,rated}} \\ &+ P_{cu,eddy,pu} \frac{235 + \theta_{hs,rated}}{235 + x_{\theta,hs}(k)}. \end{aligned} \quad (13)$$

5.1 Simulation of the thermal model

The models (10) and (12) are simulated for the 250 MVA ONAF (Oil Natural Air Forced)-cooled transformer presented in [3] and [6]. The parameters of the model are given in Table 2.

The model is simulated for a constant ambient temperature of 25.6 °C. The load profile of the transformer for the simulation is 1.0 pu for 190 minutes, 0.6 pu for 175 minutes, 1.5 pu for 145 minutes, 2.1 pu for 25 minutes and 0.0 pu for 15 minutes.

Table 2: Parameters of the 250 MVA transformer used in the case study [3,6].

| Parameter | Value |
|---------------------------------------|--------|
| $\theta_{oil,rated} / ^\circ\text{C}$ | 75 |
| $P_{cu,dc} / \text{W}$ | 411780 |
| $P_{cu,eddy} / \text{W}$ | 29469 |
| P_s / W | 43391 |
| $\Delta\theta_{hs,rated} / \text{K}$ | 20.3 |
| $\Delta\theta_{oil,rated} / \text{K}$ | 38.3 |
| $\tau_{wdg,rated} / \text{min}$ | 6 |
| M_{FLUID} / kg | 73887 |
| R | 1000 |
| n | 0.25 |
| $\theta_{oil,i} / ^\circ\text{C}$ | 38.3 |
| $\theta_{hs,i} / ^\circ\text{C}$ | 38.3 |

The top-oil and the hot-spot temperatures from the simulation are shown in Figure 4, which is similar to the results reported in [3] and [6].

6 Loading of the transformer based on the hot-spot temperature

The loading based on the hot-spot temperature is depicted in Table 1. The type of loading and the allowed limits depend on the preference of the utilities, the criticality of the transformer and the situation (e.g., under emergency conditions limits may be relaxed). The normal life expectancy loading based on the hot-spot temperature prediction (in which the maximum hot-spot temperature is maintained below 120 °C) is considered in this section.

The load of the transformer depends on the energy demand and production. A prediction of the load can be made based on the predicted generation, the predicted loading and the network configuration. For the predicted loading, the hot-spot temperature should be below the maximum value of 120 °C for the normal life expectancy loading. In the case of thermal overloading of the transformer, the load should be reduced. The load can be varied using different methods, such as network re-configurations, changing the generation and the load, using an energy storage, etc.

In our framework, the required loading is considered as reference loading $u_{I,ref}$. The actual loading of the transformer u_I should follow the reference loading within the given thermal limit of the transformer. Assuming the loading u_I to be controllable, the op-

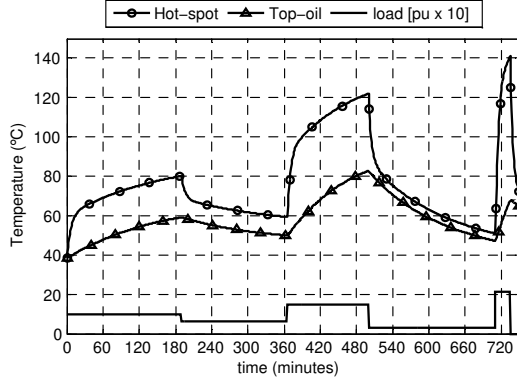


Figure 4: Hot-spot and top-oil temperatures for the given load profile.

timization problem is specified as:

$$\min_{u_1(k), \dots, u_1(k+N-1)} \sum_{l=0}^{N-1} |u_1(k+l) - u_{1,\text{ref}}(k+l)| \quad (14)$$

subject to

$$\begin{aligned} x_{\theta,\text{oil}}(k+l+1) &= f_{\text{oil}}(x_{\theta,\text{oil}}(k+l), u_1(k+l), u_{\theta,\text{amb}}(k+l)) \\ x_{\theta,\text{hs}}(k+l+1) &= f_{\text{hs}}(x_{\theta,\text{hs}}(k+l), x_{\theta,\text{oil}}(k+l), u_1(k+l)) \\ x_{\theta,\text{hs}}(k+l) &\leq 120^\circ\text{C} \quad \text{for } l = 0, \dots, N-1. \end{aligned}$$

where f_{oil} and f_{hs} are given by (10) and (12), respectively.

The optimization problem (14) consists of non-linear constraints. The optimization therefore is solved by a non-linear solver, SNOPT [9]. This solver is used through the Tomlab v6.1 [10] interface in Matlab v7.5.

6.1 Simulation of loading based on the hot-spot temperature

The 250 MVA transformer mentioned in the previous section is considered for the case study. A loading of 1.5 pu for a duration of 180 minutes is considered. The loading is considered to decrease to 0.3 pu after 180 minutes. An initial hot-spot temperature of 59.4°C and an initial top-oil temperature of 49.8°C are assumed for the case study. The assumptions are based on the temperatures at 365 minutes for the simulation presented in Section 5.1 (see Figure 4).

The hot-spot and top-oil temperature for the given conditions is shown in Figure 5. As seen in the figure, the hot-spot temperature exceeds the limit of 120°C after 120 minutes.

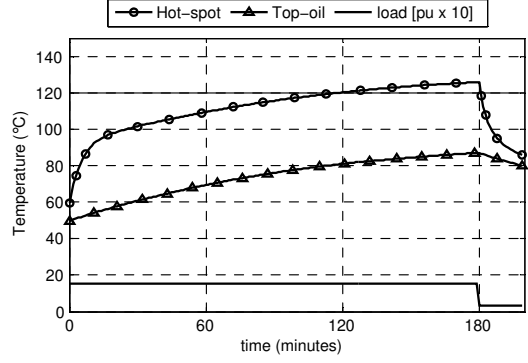


Figure 5: Hot-spot and top-oil temperatures without load control. The hot-spot temperature exceeds the limit of 120°C .

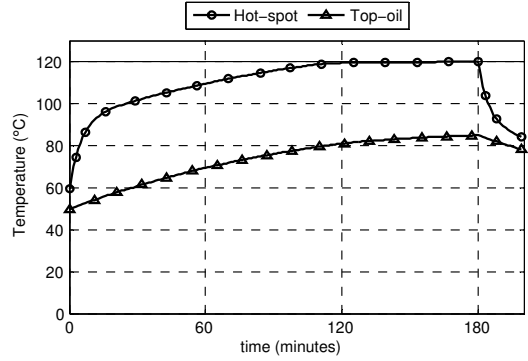


Figure 6: Hot-spot and top-oil temperatures with load control. The hot-spot temperature is maintained below the limit of 120°C .

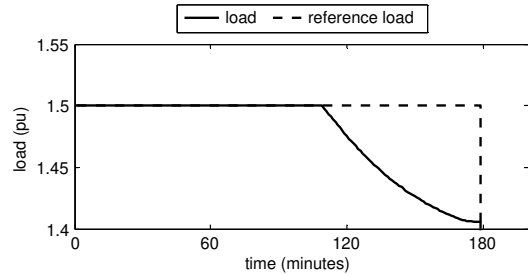


Figure 7: Load profile for the proposed load control.

Optimization of the load given in (14) is applied for the transformer. The length of the time frame over which predictions are made is 15 minutes. At each time step, the hot-spot temperature is predicted for the given prediction horizon. The optimal load profile is recommended based on the prediction. The load of the transformer is adjusted based on the recommended profile. The temperatures and the load are shown in Figure 6 and Figure 7, respectively. As seen in these figures, the hot-spot tem-

perature is kept below the limit by lowering the load of the transformer. The deviation of the load from the reference load starts at 105 minutes as the model predicts that the hot-spot temperature will exceed the limit in the predicted time frame (15 minutes).

7 Conclusions and future work

A model-based predictive optimization framework has been applied for the optimization of the loading of a transformer. By using the optimized loading profile, the hot-spot temperature was maintained below the allowed limit. The proposed method optimizes the utilization of the transformer by recommending load changes when required and by keeping the temperature within the safe limits. The effectiveness of the proposed solution depends on the accuracy of the temperature estimation and the ability to control the load of the transformer as recommended.

The framework is implemented for the normal life expectancy loading of the transformer. The planned loading beyond nameplate, long-time emergency loading and short-time emergency loading will be considered in future work. In these cases, the risk due to loading will be accounted for by considering the degree of polymerization of the paper insulation.

8 Acknowledgments

This research is supported by the SenterNovem Sinergie project EOSLT04034, the BSIK project “Next Generation Infrastructures (NGI)”, the Delft Research Center Next Generation Infrastructures, the European STREP project “Hierarchical and distributed model predictive control (HDMPC)” and the project “Multi-Agent Control of Large-Scale Hybrid Systems” (DWV.6188) of the Dutch Technology Foundation STW.

9 References

- [1] N. Dominelli, A. Rao, P. Kundur, “Life extension and condition assessment: Techniques for an aging utility infrastructure”, *IEEE Power and Energy Magazine*, vol. 4, no. 3, pp. 24–38, May–June 2006.
- [2] G. Bajracharya, T. Koltunowicz, R. R. Negenborn, Z. Papp, D. Djairam, B. De Schutter, J. J. Smit, “Optimization of Maintenance for Power

System Equipment Using a Predictive Health Model”, Technical report, Department of High-voltage Components and Power Systems, Delft University of Technology, Delft, The Netherlands, February 2009. Submitted to a conference.

- [3] Power transformers – Part 7: Loading guide for oil-immersed power transformers, IEC Standard 60076-7-2008, December 2008.
- [4] IEEE Guide for Loading Mineral-Oil-Immersed Transformers, IEEE Standard C57.91-1995, June 1995.
- [5] G. Swift, T. S. Molinski, W. Lehn, “A Fundamental Approach to Transformer Thermal Modeling, Part I: Theory and Equivalent Circuit”, *IEEE Transactions on Power Delivery*, vol. 16, no. 2, pp. 171–175, April 2001.
- [6] D. Susa, M. Lehtonen, H. Nordman, “Dynamic Thermal Modelling of Power Transformers”, *IEEE Transactions on Power Delivery*, vol. 20, no. 1, pp. 197–204, January 2005.
- [7] D. Susa, Dynamic Thermal Modelling of Power Transformers, PhD dissertation, Department of Electrical and Communications Engineering, Helsinki University of Technology, Finland, August 2005.
- [8] A. M. Emsley, G. C. Stevens, “Kinetics and mechanisms of the low temperature degradation of cellulose”, *Cellulose*, vol. 1, no. 1, pp. 26–56, March 1994.
- [9] R. Fletcher, S. Leyffer, “Nonlinear programming without a penalty function”, *Mathematical Programming*, vol. 91, no. 2, pp. 239–269, January 2002.
- [10] K. Holmström, A. O. Göran, M. M. Edvall, “User’s Guide for Tomlab/SNLP”, February 2008.